UNIVERSITY OF LEEDS

Article:
Jenkins, AKL and Forster, PM (2013) The inclusion of water with the injected aerosol reduces the simulated effectiveness of marine cloud brightening. Atmospheric Science Letters, 14 (3). 164 - 169. ISSN 1530-261X

https://doi.org/10.1002/asl2.434

This is a post-print copy of an article that is published in full by Atmospheric Science Letters
http://onlinelibrary.wiley.com/doi/10.1002/asl2.434/abstract/
Jenkins, A. K. L. and Forster, P. M. (2013), The inclusion of water with the injected aerosol reduces the simulated effectiveness of marine cloud brightening. Atmosph. Sci. Lett., 14: 164¯169. doi: 10.1002/asl2.434

The inclusion of water with the injected aerosol reduces the simulated effectiveness of marine cloud brightening

Short title: Including water in marine cloud brightening aerosol injection

A. K. L. Jenkins[1] and P. M. Forster[1]

[1] School of Earth and Environment, University of Leeds, Leeds, United Kingdom

Correspondence to:

A. K. L. Jenkins

School of Earth and Environment

The University of Leeds

Leeds

LS2 9JT

United Kingdom

eeaklj@leeds.ac.uk

+44(113) 343 9085

Abstract

Sea-salt aerosols proposed for injection in marine cloud brightening geoengineering would likely result from evaporation of sea-water droplets. Previous simulations have omitted this mechanism. Using the WRF/Chem model in large-eddy simulation mode, we find that droplet evaporation creates cold pools, suppressing initial aerosol plume heights by up to 30% (40 m). This lessens cloud albedo increases from 94.1% to 88.5% in our weakly precipitating case and from 4.3% to 1.4% for daytime injection into our non-precipitating case (cloud albedo differences of 0.012 and 0.009 respectively).

Inclusion of this effect in future modelling would allow increasingly realistic effectiveness estimates.

Keywords: marine cloud brightening; cloud seeding; WRF/Chem; marine stratocumulus; LES; cold pools, geoengineering

Introduction

The marine cloud brightening (MCB) geoengineering scheme proposes to increase the albedo of low lying marine clouds via the release of sea-salt aerosols near the sea-surface (Latham, 1990, Latham, 2002, Latham et al., 2012). Whilst real-world aerosol formation mechanisms are still being developed (Salter et al., 2008, Latham et al., 2012), it is likely that these aerosols would be formed through the evaporation of sea-water droplets emitted from wind-powered vessels (Salter et al., 2008, Latham et al., 2012). The resulting indirect aerosol effect and associated negative radiative forcing could create a cooling effect that might partially ameliorate future greenhouse gas driven warming (Lenton and Vaughan, 2009).

Owing to the potentially high risks and complexity of governance associated with geoengineering field trials, estimates of the potential effectiveness of MCB rely on model simulations. Initial global simulations omitted any representation of aerosol increase, instead modelling the brightening mechanism as a direct increase in cloud droplet number concentration (CDNC) (Latham et al., 2008, Rasch et al., 2009, Jones et al., 2009). Subsequently, developments have been made in the more realistic representation of MCB aerosol emissions (e.g. Korhonen et al., 2010). This has permitted the inclusion of increasingly complex mechanisms including: aerosol transport, processing and activation (Korhonen et al., 2010, Alterskjær et al., 2012); direct and indirect aerosol effects (Jones and Haywood, 2012, Partanen et al., 2012); and the use of earth-system models to simulate global feedbacks on meteorology and the biosphere (Jones and Haywood, 2012). Detailed consideration of the cloud response to MCB sea-salt aerosol emissions has also been undertaken at the cloud-resolving model scale (Wang et al., 2011). Such models explicitly represent cloud processes that are parameterised within global models and permit investigation of the sensitivity of a range of cloud conditions to MCB. The higher resolution also allows the representation of point-source emissions of the sea-salt aerosols and the simulation of complex dynamical feedbacks (Wang and Feingold, 2009a, Wang and Feingold, 2009b).

Whilst modelling simulations now explicitly represent the emission of MCB sea-salt aerosols, all continue to omit the water portion of the injected sea-water droplets that would likely be

present in real-world emissions. Hence they also omit the latent heat fluxes associated with droplet evaporation and the resulting buoyancy and dynamical changes that may affect the vertical transport of the emitted aerosols.

For the first time, we investigate the effect of including water in the MCB sea-salt aerosol emission on the vertical transport of aerosols through the boundary layer and the resulting cloud albedo changes. We consider this for both a non-precipitating (NP) and a weakly-precipitating (WP) marine stratocumulus cloud regime, injecting aerosol at different times of day. We focus here on the rapid cloud response. Investigation of regional scale feedbacks arising from the addition of water to the spray assumption is outside the scope of this work.

Methods

We used the Weather Research and Forecasting model coupled with Chemistry (WRF/Chem) in large-eddy simulation configuration. Aerosol processes were incorporated through the 8-bin MOSAIC scheme (Zaveri et al., 2008) with activation of aerosols to cloud droplets using the Abdul-Razzak and Ghan (2000) method. The horizontal domain size was chosen to be 9 km x 9 km, with 300 m horizontal grid spacing and periodic boundary conditions. Simulations extended 1.5 km vertically, with 50 vertical layers each approximately 30 m in height.

Two control cases were developed based on input soundings from Research Flight 02 of the DYCOMS-II field campaign which observed drizzling stratocumulus (Ackerman et al., 2009): a non-precipitating regime (NP) initialised with polluted background aerosol distribution; and a weakly-precipitating regime (WP) initialised with a relatively clean background aerosol distribution. Further details of the model set-up and control cases are described in Jenkins et al.(2013) (as cases NP-Pa and WP respectively). Briefly, the inversion height was initialised at 795 m, with large-scale divergence of 3.75×10^{-6} s^{-1}. Large-scale horizontal wind speeds were initialised at zero (following Wang and Feingold, 2009a and Wang et al., 2011). At 03:00 LT (local time), clouds in the WP simulation were ~400 m thick, with a surface precipitation rate of 0.2 mm day^{-1}, cloud fraction of 50% and cloud droplet numbers (N_d) of ~10 cm^{-3}. At 03:00 LT, the clouds in the NP simulation were ~300 m thick, with 100% cloud fraction and N_d of ~200 cm^{-3}. Both regimes exhibit a diurnal cycle in both boundary layer dynamics and cloud properties with the cloud dissipating as turbulence (resulting from cloud-top radiative cooling) diminishes into the day. For example, the cloud thins to ~150 m at 15:00 LT in the NP control simulation, with the cloud fraction reducing to ~10%. Both simulated clouds demonstrate

dynamical and microphysical behaviour typical of marine stratocumulus cloud decks (discussed further in Jenkins et al. (2013)). This includes a distribution of vertical velocity variance (an indicator of boundary layer mixing) that is stronger in the upper half of the boundary layer, characteristic of cloud-top originating buoyancy (Wood, 2012). The strength of this variance decreases into the daytime in response to the offsetting of the turbulence inducing cloud-top long-wave cooling by short-wave radiative warming.

Aerosol injections simulated a spraying vessel that would travel the length of the domain once, at a speed of 5 m s^{-1}. The injection track was along the middle of the domain in the x-direction. This track started and ended in the centre of the domain. The moving aerosol injection was simulated as an increase in Na and Cl aerosol in one base-layer grid cell at a time. Owing to the unnaturally high local aerosol emission causing unphysical model outputs from the short-wave radiation scheme, and ultimately model failure, a reduced sea-water injection rate of 7.5 kg s^{-1} was used (i.e. one quarter of the 30 kg s^{-1} proposed by Salter et al. (2008).

Aerosols within the model are either unactivated interstitial aerosols, or activated in the cloud phase. The simulated emission of dry aerosol particles (hereinafter denoted as DRY) used Na and Cl mass fluxes of 1109 and 1710 μg m^{-2} s^{-1} respectively (corresponding to the 7.5 kg s^{-1} sea-water injection rate with assumed salinity of 35 g of sea-salt per litre of sea-water), with a number flux of 0.31×10^{12} m^{-2} s^{-1}. These aerosols, simulating a dry diameter of 200 nm, were emitted into the interstitial aerosol bin size 3 (dry diameter range of 156 nm to 313 nm).

The simulation of the emission of sea-water droplets (hereinafter denoted as WET), utilised the model cloud phase, and thus included microphysical processes (for example, evaporation and coalescence). Aerosols were introduced into the cloud phase with mass and number fluxes as in the DRY case. Water was introduced into the cloud phase with a mass flux of 7.5 kg s^{-1} and number concentration equal to that of the aerosols, simulating sea-water droplets of 800 nm diameter (as suggested by Salter et al. (2008)).

Post-injection analysis was restricted to 5 hours subsequent to injection in order to avoid the effects of aerosol interference at the periodic boundaries.

Based on the hypothesis that the evaporative cooling of the sea-water droplets (and resulting negative buoyancy) affects the aerosol plume height achieved, an additional set of experiments was carried out. DRY aerosols were injected for one minute into the centre lowermost grid cell of the NP regime at 03:00 LT coincident with a temperature perturbation ranging from -0.1 K to -2 K. Thus the effects of a temperature perturbation were isolated from the effects of

increases in specific humidity. The subsequent plume heights were then analysed. These temperature perturbations are approximately equivalent to the cooling associated with sea-water injection rates of 2 kg s^{-1} to 45 kg s^{-1} assuming evaporation within one grid cell (between 0.07 and 1.5 times the emission rate proposed by Salter et al. (2008).

Results

The WET simulations did not produce any additional precipitation or wet deposition of aerosols, with emitted water droplets evaporating within one 2 second model time step in all cases. This water droplet evaporation resulted in a cooling and moistening of the lowest model layer, in grid cells local to the injections. Potential temperatures decreased by roughly 0.3 K in all WET simulations. A maximum moisture increase of 0.1 $g/kg_{dry\ air}$ occurred for aerosol injections at 03:00 LT into the WP and NP regimes (increasing background levels by approximately 1%). As a result, cold pools – regions of negative buoyancy in excess of -0.005 m s^{-2} (Tompkins, 2001; Devine, 2007) – and associated flow patterns were formed along the injection path (Figure 1). These cold pools were short-lived, dissipating within approximately 1.5 hours of the WET aerosol injection (Figures 1, 2a, 2d). In contrast, the DRY aerosol emissions produced no temperature, moisture or buoyancy changes and as such, the WET simulation aerosols remained lower in the boundary layer (Figure 2). The aerosol plumes in the WET simulations were suppressed to between 70% and 78% of the heights reached by the DRY aerosol plumes in the first hour after injection (height reductions of between 33.2 m and 46.0 m; Figure 3a).

The set of DRY experiments initialised with forced temperature perturbations similarly show suppression of the aerosol plume height (Figure 3b). The proportional plume height associated with a temperature perturbation similar to those in the WET simulations (i.e. about 0.3 K) was 72%, fitting well with the plume height suppressions seen in the WET simulations themselves. This supports the idea that it is the temperature decreases resulting from evaporative cooling of the sea-water droplets that affects the aerosol plume height achieved, rather than changes to the moisture profile resulting from the addition of water.

Although the cold pools were short-lived, the height suppression of the WET simulation aerosols continued for the duration of the simulations (Figure 2 c, f). As such, the number of emitted aerosols reaching the cloud base was smaller in all WET cases compared to DRY. This difference was dependent on regime and injection time (Figure 4 a, b, c, d). We consider first the NP regime. For injection at 03:00 LT, the number of aerosols reaching the cloud base was

consistently halved for the WET compared to DRY injections (reaching domain averages of 62 cm^{-3} and 125 cm^{-3} respectively by the end of the simulations; Figure 4a). For injection at 08:00 LT into the increasingly uncoupled boundary layer, the number of aerosols reaching cloud base was small for both WET and DRY injections (fewer than 10 cm^{-3} averaged over the domain; Figure 4b). While aerosols injected at 03:00 LT began to reach the cloud base after one hour (Figure 4a), DRY aerosols injected at 13:00 LT took around two hours to begin to reach the cloud base (Figure 4c). WET aerosols injected at 13:00 LT, took approximately three hours to begin to reach the cloud base (Figure 4c). By the end of the 13:00 LT simulations, the increase in aerosol number concentration of bin 3 aerosols (the injected aerosol size) just below the cloud base was approximately 170 cm^{-3} for the DRY and 50 cm^{-3} for WET injections.

In terms of albedo increases (Figure 4 e, f, g, h), injection at 13:00 LT into the NP cloud showed most sensitivity to the WET/DRY aerosol assumption. Here, the average cloud albedo over the 5 hour simulation increased by 0.014 (4.3%) for the DRY injection but by only 0.005 (1.4%) in response to the WET injection (Figure 4g). Including water in the simulated aerosol injection therefore lessened the cloud albedo increase by 67%.

For injection at 03:00 LT, the cloud albedo increased by 0.018 (2.9%) for the DRY injection and by 0.012 (1.9%) for the WET injection (Figure 4e). For injection at 08:00 LT into the increasingly uncoupled boundary layer, the cloud albedo increases were 0.002 (0.6%) for the DRY injection and 0.001 (0.3%) for the WET (Figure 4f).

For injection at 03:00 LT into the WP regime, the average increase in cloud albedo was 0.160 (94.1%) for the DRY injection and 0.148 (88.5%) for the WET (Figure 4h). So, whilst including water in the simulated aerosol injection lessens the cloud albedo increase by only 7.5%, this equates to an absolute difference in cloud albedo increase of 0.012. This is larger than the 0.009 difference in cloud albedo increase for NP 13:00 LT injections.

Discussion and conclusions

The speed at which droplets evaporate within our simulations is consistent with calculations for similarly sized droplets (Lewis and Schwartz, 2004). The absence of sufficient water droplet coalescence to cause the loss of aerosols through wet deposition may however be a consequence of the initial dispersal of the injected droplets within our grid cell. Whilst model grid cell spacings of hundreds of metres are able to resolve cloud processes (Wang and Feingold, 2009a), they are too coarse to capture the detailed emission processes occurring from

a proposed rotor diameter of 2.4 m (Salter et al., 2008). Further investigation of these processes may be suited to a plume aerosol model that follows a parcel of the emitted aerosols as it expands, enabling a range of processes to be captured at relevant resolutions during plume growth (e.g. Pierce et al., 2010).

The initial suppression of WET aerosol plume heights was fairly uniform across all regimes and injection times (Figure 3a). Our analysis suggests that subsequent differences in the plume heights, CDNC and albedo response for the NP regime are related to the turbulent structure of the boundary layer through the diurnal cycle, and are hence dependent on time of injection. This is represented schematically in Figure 5. The turbulent structure of the system is illustrated by the resolved turbulent kinetic energy (TKE). Whilst turbulence is maintained throughout the boundary layer, its distribution varies over the diurnal cycle. Early in the morning, turbulence that originates from cloud-top long-wave radiative cooling penetrates deep into the boundary layer, meeting turbulent mixing in the layer near the surface that results from surface fluxes and wind shear. In this coupled state, aerosols are able to be drawn up to the cloud. It is proposed that since the WET aerosol plume height is suppressed compared to the DRY case, more aerosols stay closer to the surface, and thus fewer are drawn to the cloud base, resulting in smaller albedo increases (cf. Figure 4 a, e). Into the day, as solar heating offsets the cloud-top originating production of turbulence, the depth of cloud-originating TKE penetration decreases, and the boundary layer becomes uncoupled. Thus, whilst mixing of the aerosol plumes still occurs close to the surface for injection at 08:00 LT, the lack of coupling to the cloud region mixed layer inhibits transport of the aerosols up to the cloud region, and hence little albedo change occurs (cf. Figure 4 b, f). Into the evening, solar heating of the cloud diminishes and the strength of turbulent production at the cloud top increases. Whilst the cloud and boundary layers remain poorly coupled at the time of 13:00 LT aerosol injection, after approximately two hours, the cloud-top originating turbulence has penetrated deep enough into the boundary layer to coincide with the mixed region of DRY aerosols, thus transporting them up to the cloud layer. Owing to the suppression in plume height characteristic to the WET aerosol assumption, aerosols are not drawn up into the cloud layer until further deepening and recoupling of the cloud and boundary layers has occurred. This occurs approximately one hour later than for the DRY assumption (cf, Figure 4 c, g).

As the magnitude of albedo perturbation is dependent on aerosol height, they are also sensitive to the aerosol emission height assumption. For injection into the second model layer from

bottom for the NP regime, the maximum difference in mean albedo perturbation between the WET and DRY simulations increases to 0.011 (from 0.009 for injection into the bottom layer).

Whilst our simulations provide estimates of the sensitivity to the WET/DRY assumption for both non-precipitating and weakly precipitating cloud regimes, we acknowledge that our simulations represent only a small subset of potential conditions encountered in marine stratocumulus cloud regions. For example, the low cloud base in our WP regime allowed a sufficient number of aerosols to reach the cloud base to instigate a strong second indirect effect in both WET and DRY cases. This resulted in a relatively small percentage difference in cloud albedo increase. The sensitivity to the WET/DRY assumption may increase for weakly precipitating clouds with higher cloud bases as the vertical gradient of injected aerosols becomes more important. Future experiments, exploring the sensitivity of aerosol transport to the cloud under a range of atmospheric conditions including moisture and temperature profiles, large-scale divergence rates, wind speeds and inversion heights would be of interest. The relative humidity of the boundary layer will also affect the rate of evaporation of injected droplets, affecting temperature perturbations and resulting plume suppression.

Our simulations use injection rates equivalent to one quarter of those suggested by Salter et al. (2008). The DRY experiments initialised with forced temperature perturbations suggest that the greater evaporative cooling associated with increased sea-water injection rates may lead to the aerosol plumes being suppressed by up to 46% (Figure 3b). This larger disparity between initial injected aerosol plume heights may lead to more significant sensitivities across many of the cases (although the daytime injections would likely remain relatively insensitive).

In this study, we have shown that the cooling associated with the evaporation of injected sea-water droplets should be accounted for in future MCB assessments. We suggest that the development of a parameterisation of this phenomenon for use in global scale models, or the explicit representation of this additional water in cloud resolving models would contribute towards increasingly realistic estimates of MCB effectiveness.

Acknowledgements

This research was funded by the EPSRC and NERC through the 'Integrated Assessment of Geoengineering Proposals' (IAGP, http://www.iagp.ac.uk). P.M.F. is additionally supported by a Royal Society Wolfson Merit Award. A.K.L.J is supported through a Met Office CASE

studentship. Kirsty Pringle provided GLOMAP data and Douglas Lowe and the Manchester group provided the sea-salt emission parameterisation and model advice.

Abdul-Razzak, H & Ghan, SJ 2000. A parameterization of aerosol activation 2. Multiple aerosol types. *J. Geophys. Res.,* 105**,** 6837-6844 DOI:10.1029/1999jd901161

Ackerman, AS, Vanzanten, MC, Stevens, B, Savic-Jovcic, V, Bretherton, CS, Chlond, A, Golaz, J-C, Jiang, H, Khairoutdinov, M, Krueger, SK, Lewellen, DC, Lock, A, Moeng, C-H, Nakamura, K, Petters, MD, Snider, JR, Weinbrecht, S & Zulauf, M 2009. Large-Eddy Simulations of a Drizzling, Stratocumulus-Topped Marine Boundary Layer. *Monthly Weather Review,* 137**,** 1083-1110 DOI:10.1175/2008MWR2582.1

Alterskjær, K, Kristjánsson, JE & Seland, Ø 2012. Sensitivity to deliberate sea salt seeding of marine clouds – observations and model simulations. *Atmospheric Chemistry and Physics,* 12**,** 2795-2807 DOI:10.5194/acp-12-2795-2012

Jenkins, AKL, Forster, PM & Jackson, LS 2013. The effects of timing and rate of marine cloud brightening aerosol injection on albedo changes during the diurnal cycle of marine stratocumulus clouds. *Atmospheric Chemistry and Physics,* 13**,** 1659-1673 DOI:10.5194/acp-13-1659-2013

Jones, A, Haywood, J & Boucher, O 2009. Climate impacts of geoengineering marine stratocumulus clouds. *J. Geophys. Res.,* 114**,** D10106 DOI:10.1029/2008jd011450

Jones, A & Haywood, JM 2012. Sea-spray geoengineering in the HadGEM2-ES earth-system model: radiative impact and climate response. *Atmospheric Chemistry and Physics,* 12**,** 10887-10898 DOI:10.5194/acp-12-10887-2012

Korhonen, H, Carslaw, KS & Romakkaniemi, S 2010. Enhancement of marine cloud albedo via controlled sea spray injections: a global model study of the influence of emission rates, microphysics and transport. *Atmospheric Chemistry and Physics,* 10**,** 4133-4143 DOI:10.5194/acp-10-4133-2010

Latham, J 1990. Control of global warming? *Nature,* 347**,** 339-340 DOI:10.1038/347339b0

Latham, J 2002. Amelioration of global warming by controlled enhancement of the albedo and longevity of low-level maritime clouds. *Atmospheric Science Letters,* 3**,** 52-58 DOI:10.1006/asle.2002.0099

Latham, J, Bower, K, Choularton, T, Coe, H, Connolly, P, Cooper, G, Craft, T, Foster, J, Gadian, A, Galbraith, L, Iacovides, H, Johnston, D, Launder, B, Leslie, B, Meyer, J, Neukermans, A, Ormond, B, Parkes, B, Rasch, P, Rush, J, Salter, S, Stevenson, T, Wang, H, Wang, Q & Wood, R 2012. Marine cloud brightening. *Philosophical Transactions of the Royal Society A: Mathematical, Physical and Engineering Sciences,* 370**,** 4217-4262 DOI:10.1098/rsta.2012.0086

Latham, J, Rasch, P, Chen, C-C, Kettles, L, Gadian, A, Gettelman, A, Morrison, H, Bower, K & Choularton, T 2008. Global temperature stabilization via controlled albedo enhancement of low-level maritime clouds. *Philosophical Transactions of the Royal Society A: Mathematical, Physical and Engineering Sciences,* 366**,** 3969-3987 DOI:10.1098/rsta.2008.0137

Lenton, TM & Vaughan, NE 2009. The radiative forcing potential of different climate geoengineering options. *Atmospheric Chemistry and Physics,* 9**,** 5539-5561 DOI:10.5194/acp-9-5539-2009

Lewis, ER & Schwartz, SE 2004. *Sea Salt Aerosol Production: Mechanisms, Methods, Measurements and Models : a Critical Review*, American Geophysical Union.

Partanen, A-I, Kokkola, H, Romakkaniemi, S, Kerminen, V-M, Lehtinen, KEJ, Bergman, T, Arola, A & Korhonen, H 2012. Direct and indirect effects of sea spray geoengineering and the role of injected particle size. *J. Geophys. Res.,* 117**,** D02203 DOI:10.1029/2011jd016428

Pierce, JR, Weisenstein, DK, Heckendorn, P, Peter, T & Keith, DW 2010. Efficient formation of stratospheric aerosol for climate engineering by emission of condensible vapor from aircraft. *Geophys. Res. Lett.,* 37**,** L18805 DOI:10.1029/2010gl043975

Rasch, PJ, Latham, J & Chen, CC 2009. Geoengineering by cloud seeding: influence on sea ice and climate system. *Environmental Research Letters,* 4 DOI:10.1088/1748-9326/4/4/045112

Salter, S, Sortino, G & Latham, J 2008. Sea-going hardware for the cloud albedo method of reversing global warming. *Philosophical Transactions of the Royal Society A: Mathematical, Physical and Engineering Sciences,* 366**,** 3989-4006 DOI:10.1098/rsta.2008.0136

Wang, H & Feingold, G 2009a. Modeling Mesoscale Cellular Structures and Drizzle in Marine Stratocumulus. Part I: Impact of Drizzle on the Formation and Evolution of Open Cells. *Journal of the Atmospheric Sciences,* 66**,** 3237-3256 DOI:10.1175/2009JAS3022.1

Wang, H & Feingold, G 2009b. Modeling Mesoscale Cellular Structures and Drizzle in Marine Stratocumulus. Part II: The Microphysics and Dynamics of the Boundary Region between Open and Closed Cells. *Journal of the Atmospheric Sciences,* 66**,** 3257-3275 DOI:10.1175/2009JAS3120.1

Wang, H, Rasch, PJ & Feingold, G 2011. Manipulating marine stratocumulus cloud amount and albedo: a process-modelling study of aerosol-cloud-precipitation interactions in response to injection of cloud condensation nuclei. *Atmospheric Chemistry and Physics,* 11**,** 4237-4249 DOI:10.5194/acp-11-4237-2011

1 Wood, R 2012. Stratocumulus Clouds. *Monthly Weather Review,* 140**,** 2373-2423 DOI:10.1175/mwr-d-
2 11-00121.1

3 Zaveri, RA, Easter, RC, Fast, JD & Peters, LK 2008. Model for Simulating Aerosol Interactions and
4 Chemistry (MOSAIC). *J. Geophys. Res.,* 113**,** D13204 DOI:10.1029/2007jd008782

5

6

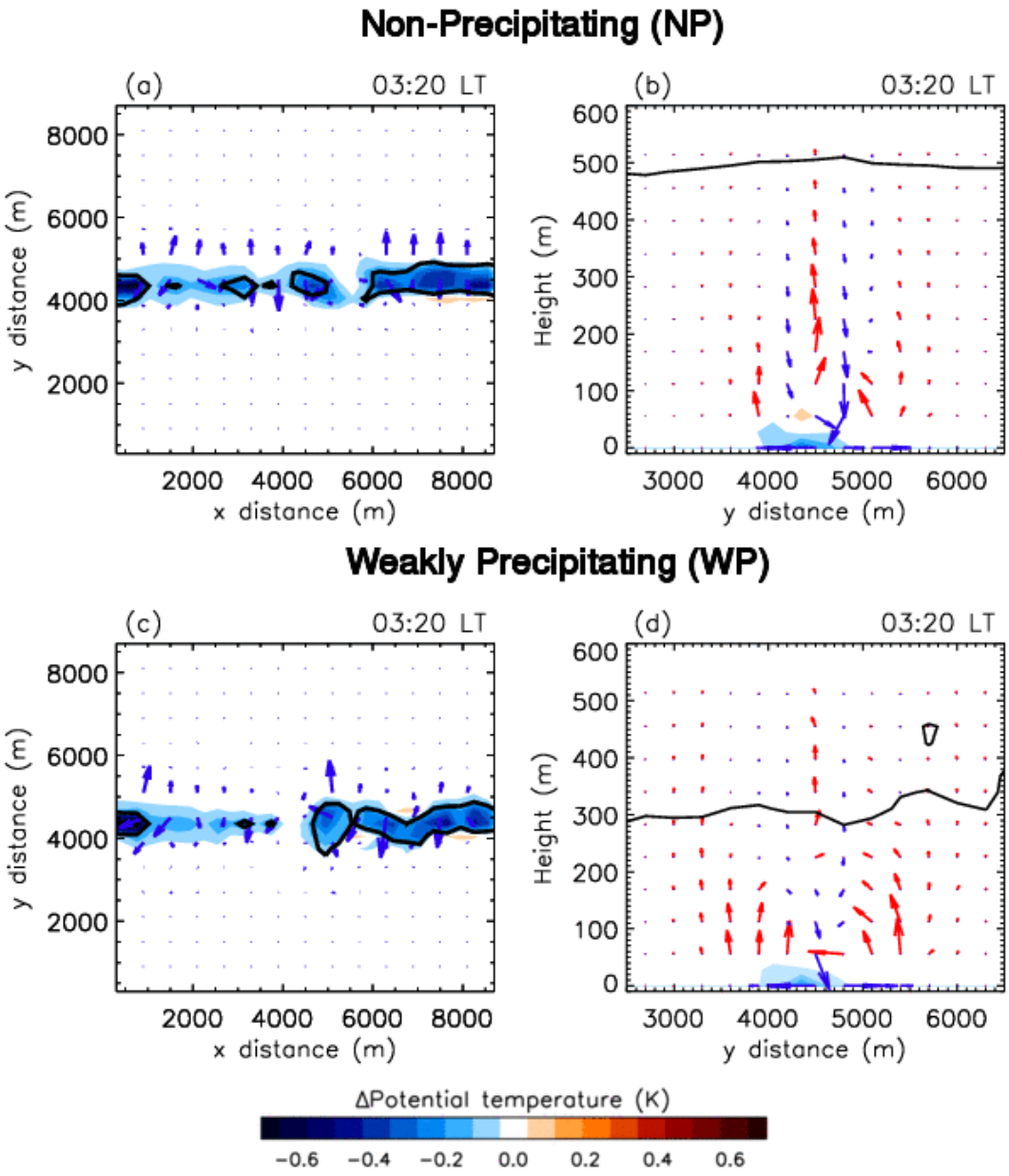

FIGURE 1 (VIDEO S1)

(a) Difference in surface potential temperature (WET minus DRY) for aerosol injection into the NP regime at 03:00 LT. Arrows show differences in surface flow patterns. Thick black contours outline cold pools (buoyancies in excess of -0.005 m s^{-2}); (b) Mean (averaged over the x-direction) of difference in potential temperature between DRY and WET aerosol injections into NP regime at 03:00 LT. Arrows show differences in mean flow patterns (red=updrafts, blue=downdrafts). Black lines show mean cloud outline; (c) As '(a)' but for WP regime for injection at 03:00 LT; (d) As '(b)' but for WP regime for injection at 03:00 LT.

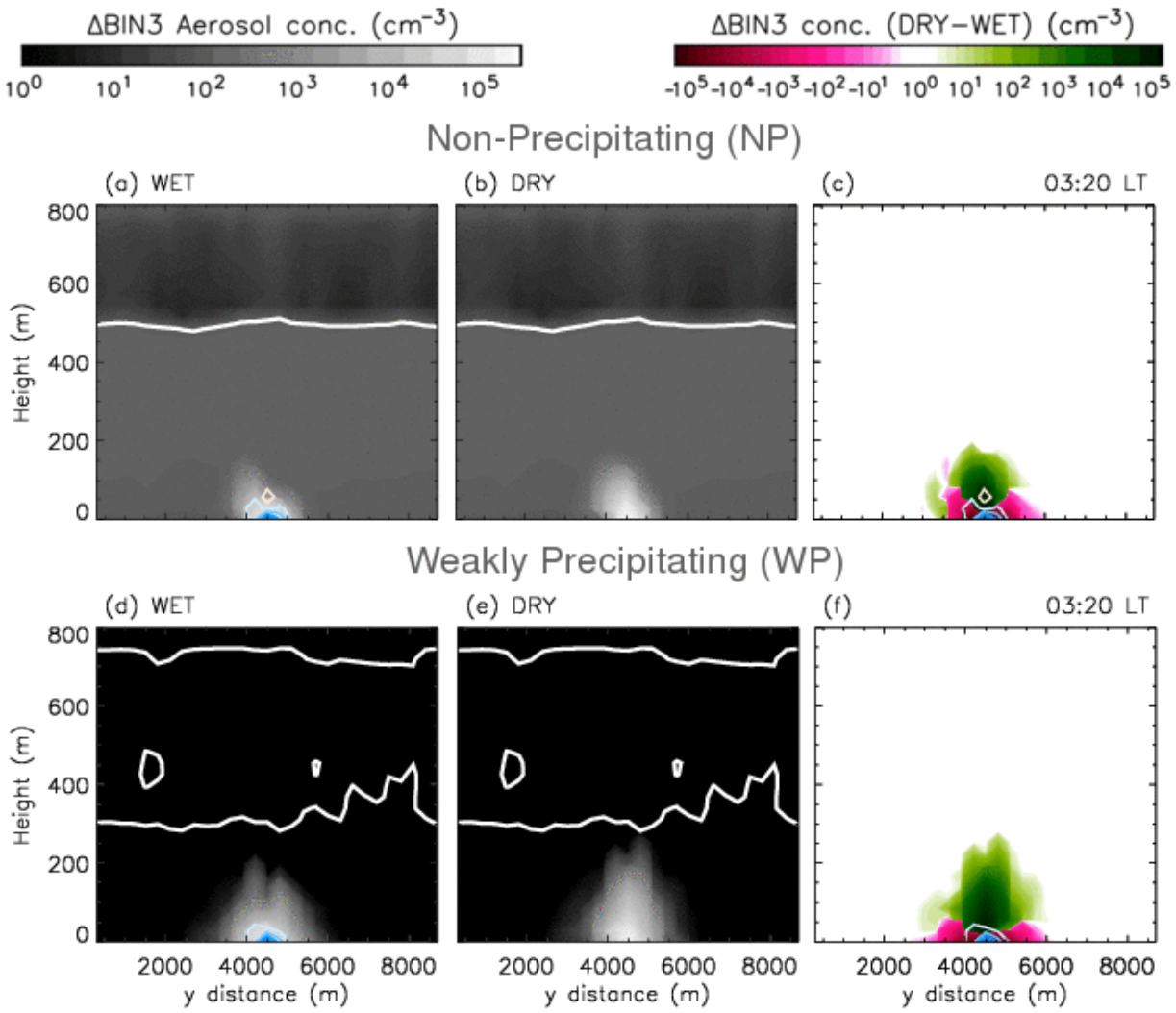

FIGURE 2 (VIDEO S2)

Progression through time for injection at 03:00 LT: (a) NP regime WET case: injected aerosol (bin 3) concentration (grey scale filled contours), perturbation of potential temperature from Control (coloured contour lines with scale as in Figure 1), and cloud top and base (thick white outline). All outputs are averaged over the x-direction; (b) as '(a)' but for NP regime DRY case; (c) NP regime: Difference in injected aerosol (bin 3) concentration between the DRY and WET simulations, and difference in potential temperature between WET and DRY injections (coloured contour lines with scale as in Figure 1); (d) as '(a)' but for WP regime, (e) as '(b)' but for WP regime, (f) as '(c)' but for WP regime.

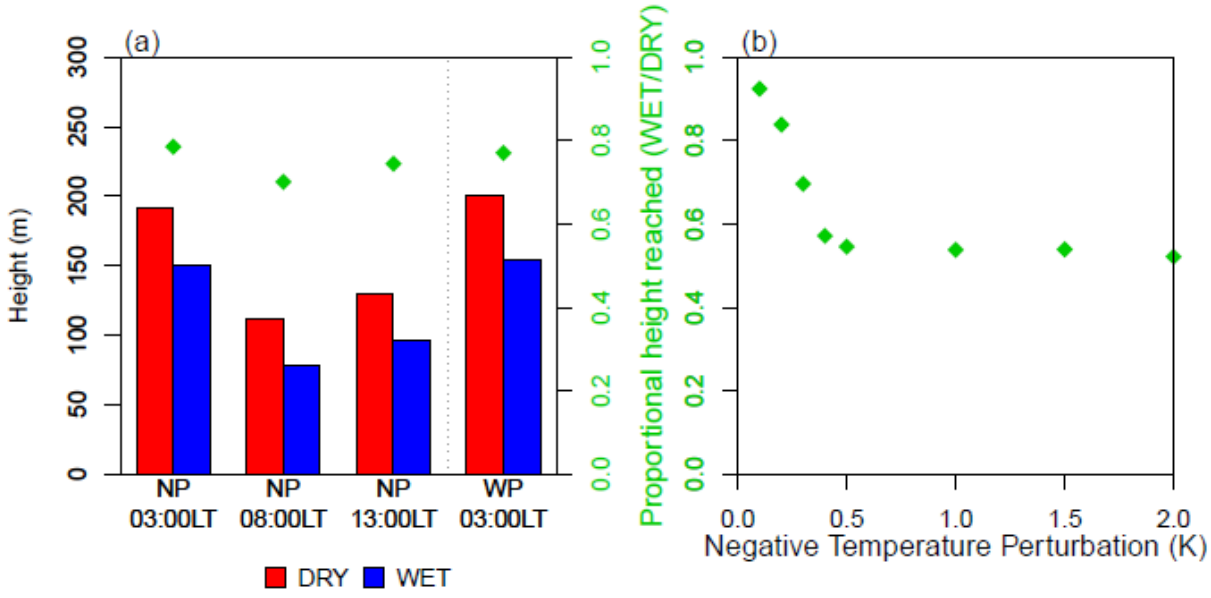

FIGURE 3

Initial aerosol plume heights: (a) Height achieved by DRY and WET aerosol plumes averaged over the first hour after injection (bars). Also shown as a proportional height, i.e. WET plume height / DRY plume height (green diamonds). Heights are taken as the 100 cm^{-3} isoline of the injected aerosol size bin (bin 3); (b) Proportional heights reached by DRY aerosol injections under forced initial negative temperature perturbations (20 minutes after injection with heights taken as the 50 cm^{-3} isoline of bin 3 aerosols)

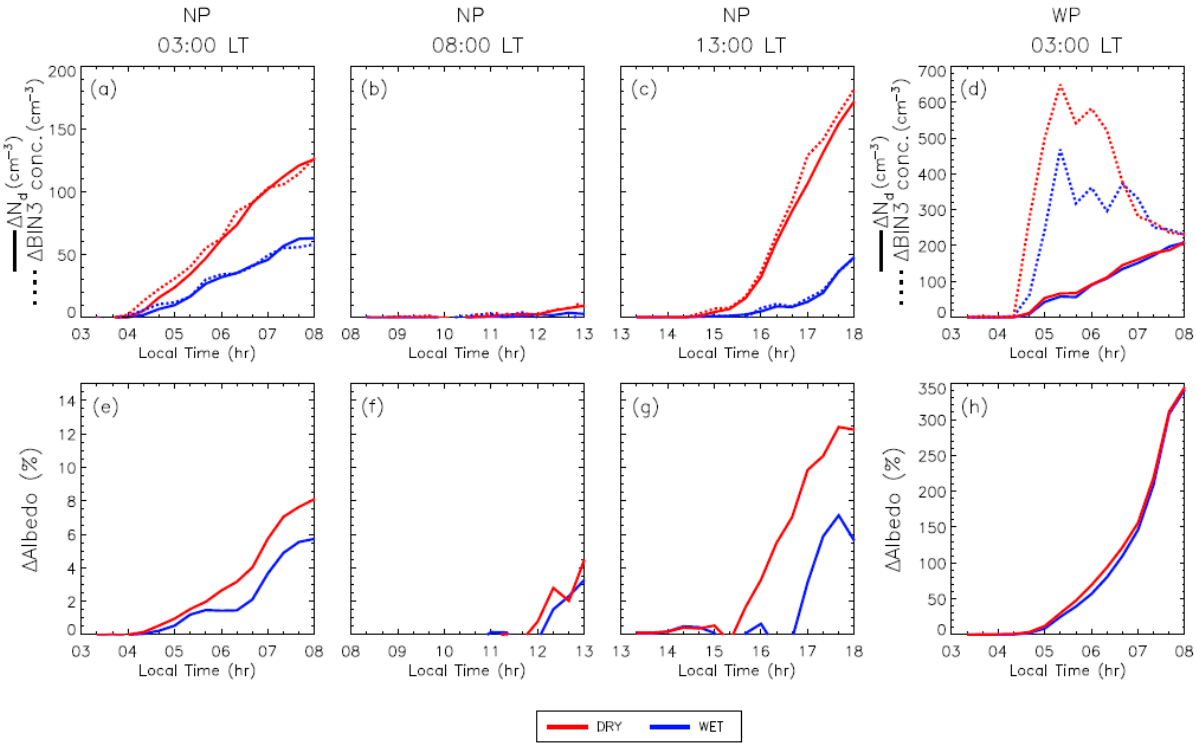

FIGURE 4

(a) Time series of the increase in domain average injected aerosol concentration in the layer below cloud base (ΔBIN3 conc; cm^{-3}; dotted line) and the increase in domain average cloud droplet number concentration (ΔN_d; cm^{-3}; solid line) for the NP regime with aerosol injection at 03:00 LT; (b) as '(a)' but for aerosol injection at 08:00 LT; (c) as '(a)' but for aerosol injection at 13:00 LT; (d) as '(a)' but for the WP regime with aerosol injection at 03:00 LT; (e) time series of the domain average albedo increase for the NP regime with aerosol injection at 03:00 LT; (f) as '(e)' but for aerosol injection at 08:00 LT; (g) as '(e)' but for aerosol injection at 13:00 LT; (h) as '(e)' but for the WP regime with aerosol injection at 03:00 LT.

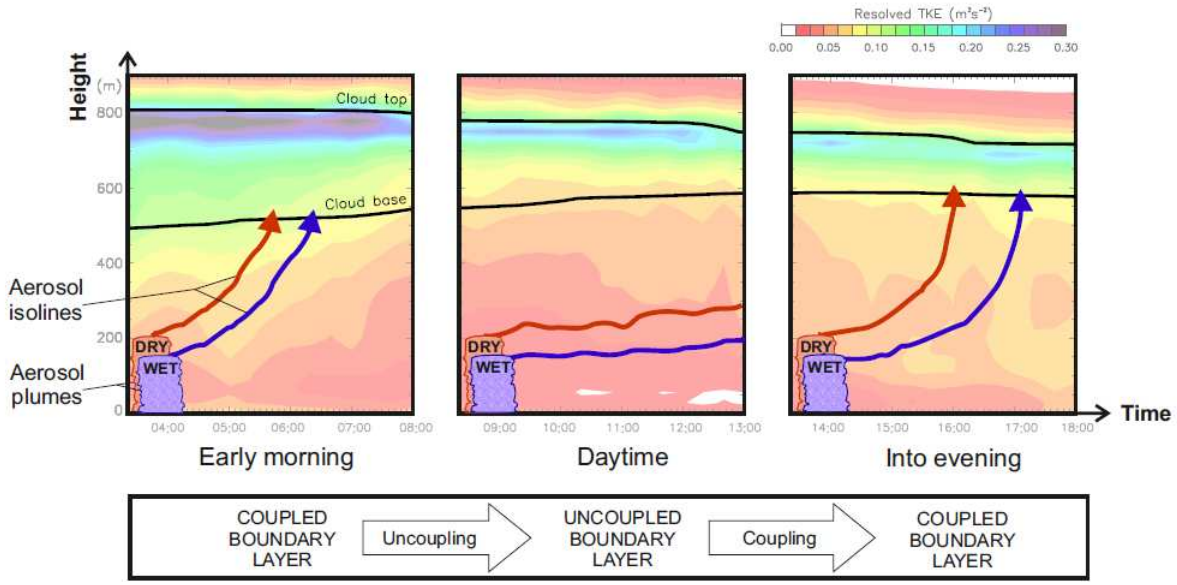

FIGURE 5

Schematic showing proposed relationship between initial WET and DRY aerosol plumes, subsequent transport of aerosols (represented by aerosol isolines) and turbulence within the marine stratocumulus topped boundary layer over time (coloured contour transparancies showing the domain average resolved turbulent kinetic energy for the NP case).